

Structural network efficiency predicts conversion to dementia

Anil M. Tuladhar, MD
Ingeborg W.M. van Uden, MD
Loes C.A. Rutten-Jacobs, PhD
Andrew Lawrence, PhD
Helena van der Holst, MD
Anouk van Norden, MD, PhD
Karlijn de Laat, MD, PhD
Ewoud van Dijk, MD, PhD
Jurgen A.H.R. Claassen, MD, PhD
Roy P.C. Kessels, PhD
Hugh S. Markus, MD, PhD
David G. Norris, PhD
Frank-Erik de Leeuw, MD, PhD

Correspondence to
Dr. de Leeuw:
frank.erik.deleeuw@radboudumc.nl

ABSTRACT

Objective: To examine whether structural network connectivity at baseline predicts incident all-cause dementia in a prospective hospital-based cohort of elderly participants with MRI evidence of small vessel disease (SVD).

Methods: A total of 436 participants from the Radboud University Nijmegen Diffusion Tensor and Magnetic Resonance Cohort (RUN DMC), a prospective hospital-based cohort of elderly without dementia with cerebral SVD, were included in 2006. During follow-up (2011–2012), dementia was diagnosed. The structural network was constructed from baseline diffusion tensor imaging followed by deterministic tractography and measures of efficiency using graph theory were calculated. Cox proportional regression analyses were conducted.

Results: During 5 years of follow-up, 32 patients developed dementia. MRI markers for SVD were strongly associated with network measures. Patients with dementia showed lower total network strength and global and local efficiency at baseline as compared with the group without dementia. Lower global network efficiency was independently associated with increased risk of incident all-cause dementia (hazard ratio 0.63, 95% confidence interval 0.42–0.96, $p = 0.032$); in contrast, individual SVD markers including lacunes, white matter hyperintensities volume, and atrophy were not independently associated.

Conclusions: These results support a role of network disruption playing a pivotal role in the genesis of dementia in SVD, and suggest network analysis of the connectivity of white matter has potential as a predictive marker in the disease. **Neurology® 2016;86:1112–1119**

GLOSSARY

AAL = automated anatomical labeling; **AD** = Alzheimer disease; **CI** = confidence interval; **DSM-IV** = *Diagnostic and Statistical Manual of Mental Disorders, 4th edition*; **DTI** = diffusion tensor imaging; **FA** = fractional anisotropy; **FLAIR** = fluid-attenuated inversion recovery; **FLIRT** = functional MRI of the brain linear image registration tool; **GM** = gray matter; **HR** = hazard ratio; **Lasso** = least absolute shrinkage and selection operator; **MD** = mean diffusivity; **MET** = metabolic equivalent value; **MMSE** = Mini-Mental State Examination; **RUN DMC** = Radboud University Nijmegen Diffusion Tensor and Magnetic Resonance Cohort; **STRIVE** = Standards for Reporting Vascular changes on neuroimaging; **SVD** = small vessel disease; **TE** = echo time; **TI** = inversion time; **TR** = repetition time; **VaD** = vascular dementia; **WM** = white matter; **WMH** = white matter hyperintensities.

Cerebral small vessel disease (SVD) is an important cause of cognitive impairment and dementia. SVD is also a common finding in elderly participants, including those with normal cognitive function. MRI features of SVD include white matter hyperintensities (WMH), lacunes of presumed vascular origin, microbleeds, and atrophy.¹ Emerging evidence suggests that SVD may interact with neurodegenerative diseases (e.g., Alzheimer disease [AD]), thereby further increasing the risk for dementia.² As dementia is a major health problem with devastating consequences for patients and caregivers, early identification of individuals at risk is important to develop effective treatment and management approaches. Conventional SVD markers and hippocampal volume are associated with cognitive decline and dementia.^{2,3} A recent study showed that the

From the Departments of Neurology (A.M.T., I.W.M.v.U., H.v.d.H., E.v.D., F.-E.d.L.), Geriatrics (J.A.H.R.C., R.P.C.K.), and Medical Psychology (R.P.C.K.), Radboudumc, and Centre for Cognitive Neuroimaging, Radboud University Nijmegen (A.M.T., D.G.N.), Donders Institute for Brain, Cognition and Behaviour, Nijmegen, Netherlands; Department of Clinical Neurosciences, Neurology Unit (L.C.A.R.-J., A.L., H.S.M.), University of Cambridge, UK; Department of Neurology (A.v.N.), Amphia ziekenhuis Breda; Department of Neurology (K.d.L.), Haga Ziekenhuis Den Haag, the Netherlands; Erwin L. Hahn Institute for Magnetic Resonance Imaging (D.G.N.), University of Duisburg-Essen, Essen, Germany; and MIRA Institute for Biomedical Technology and Technical Medicine (D.G.N.), University of Twente, Enschede, the Netherlands.

Go to Neurology.org for full disclosures. Funding information and disclosures deemed relevant by the authors, if any, are provided at the end of the article.

association of these SVD markers with cognitive impairment might at least in part be mediated by damage to the white matter (WM) network measured using diffusion tensor imaging (DTI).⁴ Network measures have been proposed as a disease marker,⁴ yet little is known about their predictive value. Here, we examine the relation between WM network efficiency and the 5-year risk of dementia in participants with SVD without dementia.

METHODS Study population. The Radboud University Nijmegen Diffusion Tensor and Magnetic resonance Cohort (RUN DMC) study prospectively investigates risk factors and clinical consequences of brain changes as assessed by MRI. This hospital-based study consists of 503 participants with SVD without dementia aged between 50 and 85 years. On the basis of established research criteria, SVD was defined as the presence of WMH or lacunes on neuroimaging.^{1,5} Symptoms of SVD include acute symptoms, such as TIAs or lacunar syndromes, or subacute manifestations, such as cognitive or motor disturbances or depressive symptoms. Baseline data collection was performed in 2006. Inclusion criteria were age between 50 and 85 years and SVD on neuroimaging (WMH or lacunes). Participants who underwent routine diagnostic brain imaging (for, among others, vascular causes [TIA, stroke], headache, mild traumatic brain injury, and cognitive complaints) were eligible for participation. Exclusion criteria were dementia; parkinson(ism); intracranial hemorrhage; life expectancy <6 months; intracranial space-occupying lesion; (psychiatric) disease interfering with cognitive or motor testing; recent or current use of acetylcholine-esterase inhibitors, neuroleptic agents, L-dopa, or dopa-agonist/antagonists; non-SVD-related WMH mimics (e.g., multiple sclerosis); prominent visual or hearing impairment; language barrier; or MRI contraindications or known claustrophobia.⁶ Follow-up was completed in 2012. Of 503 baseline participants, 2 were lost to follow-up, 49 had died, and 54 refused in-person follow-up, but clinical endpoints were available. For this study, 436 patients were included; 67 participants were excluded because of the baseline presence of territorial infarcts (n = 55), inadequate quality of the MRI (n = 4), or failure of the DTI pipeline (n = 8).

Standard protocol approvals, registrations, and patient consents. All participants signed an informed consent form. The Medical Review Ethics Committee region Arnhem-Nijmegen approved the study.

Dementia diagnosis. Clinical endpoints were available for all participants (n = 436). Dementia diagnosis was made by referring the patient to the memory clinic of Radboud Alzheimer Center or by a panel consisting of a neurologist, clinical neuropsychologist, and geriatrician reviewing all available medical records and cognitive assessments. Diagnosis was based on DSM-IV⁷ criteria; probable AD was based on National Institute on Aging–Alzheimer’s Association criteria⁸ and vascular dementia (VaD) was based on National Institute of Neurological Disorders and Stroke–Association Internationale pour la Recherche en l’Enseignement en Neurosciences criteria.⁹ The onset of dementia was defined as the date on which the clinical symptoms were compatible with the diagnosis. If the exact date was not known, the midpoint was used between the baseline visit and the first date the diagnosis was confirmed, or, failing this, the date the participant was admitted to a nursing home because of dementia.

MRI acquisition. MRI was performed on a 1.5T S Magnetom Sonata scanner (Siemens Medical Solutions, Erlangen, Germany), including T1 3D magnetization-prepared rapid gradient echo imaging (repetition time [TR] = 2.25 s, echo time [TE] = 3.68 ms, inversion time [TI] = 850 ms, flip angle [FA] = 15°, voxel size 1.0 × 1.0 × 1.0 mm), a fluid-attenuated inversion recovery (FLAIR) sequence (TR = 9.00 s, TE = 84 ms, TI = 2.20 s, voxel size 1.0 × 1.2 × 5.0 mm, plus an interslice gap of 1 mm), T2*-weighted gradient echo sequences (TR = 800 ms, TE = 26 ms, voxel size 1.3 × 1.0 × 6.0 mm, interslice gap 1 mm), and a DTI sequence (TR = 10.10 s, TE = 93 ms, voxel size 2.5 × 2.5 × 2.5 mm, 4 unweighted scans, 30 diffusion-weighted scans with b value of 900 s/mm²). All participants were scanned on the same scanner.¹⁰

Vascular risk factors. Hypertension was defined as systolic blood pressure ≥140 mm Hg or diastolic blood pressure ≥90 mm Hg or use of antihypertensive drugs. Blood pressures were measured 3 times in supine position after 5 minutes of rest. Diabetes and hypercholesterolemia were considered to be present if the participant was taking antidiabetic or lipid-lowering drugs for high cholesterol. Body mass index was calculated as weight divided by height (in meters) squared. Smoking status was obtained through standardized questionnaires, which was checked during the interview. Leisure time physical activity was assessed with a questionnaire: participants were asked to estimate the average amount of time per week during the past year spent on the physical activities.¹¹ Metabolic equivalent value (MET) was assigned to each activity. One MET is proportional to the energy expended while sitting quietly. For each activity, we estimated the energy expended in MET h/wk, by multiplying its MET value by the time spent performing it.¹¹

MRI markers. WMH were manually segmented on FLAIR images and the total WMH volume was calculated by summing the segmented areas multiplied by slice thickness. Rating of lacunes and microbleeds was revised according to the recently published Standards for Reporting Vascular changes on neuroimaging (STRIVE) by trained raters blinded to all clinical data.¹ WMH were defined as white matter hyperintensities on FLAIR images without prominent or only faint hypointensity on the T1-weighted images, except for gliosis surrounding infarcts.¹ Lacunes were defined as hypointense areas >2 mm and ≤15 mm on FLAIR and T1, ruling out enlarged perivascular spaces (≤2 mm, except around the anterior commissure, where perivascular spaces can be large) and infraputaminial pseudolacunes.¹ There were good intrarater and interrater variability with weighted kappa of 0.87 and 0.95, respectively, for the presence of lacunes and 0.85 and 0.86 for the presence of microbleeds, calculated in 10% of the scans. Interrater variability (assessed by intraclass correlation coefficient) for total WMH volume was 0.99. Automated segmentation on T1 images was performed using Statistical Parametric Mapping (SPM5) to obtain gray matter (GM), WM, and CSF probability maps. These maps were binarized and summed to supply total volumes. These volumes and WMH volume were normalized to the total intracranial volume. The b0 images were first used to compute the coregistration parameters to the skull-stripped T1 images using functional MRI of the brain linear image registration tool (FLIRT), applied to all diffusion-weighted images. Next, we calculated the mean fractional anisotropy (FA) and mean diffusivity (MD) within the whole white matter.

Network nodes (brain regions). Brain regions were demarcated by the automated anatomical labeling (AAL) template,¹² which resulted in 45 regions for each hemisphere. Cerebellar regions were excluded, because the tractography technique

employed in this study is unsuitable for tracing cerebellar connections. Using the FSL 5.0.5 tools,¹³ the skull-stripped T1 images were nonlinearly registered to Montreal Neurological Institute 152 template using functional MRI of the brain nonlinear registration tool. Next, the transformation matrix was derived from the registration of b0 images to T1 space using FLIRT. These transformations were then used to register the AAL image to each participant's diffusion image space.

Network edges (WM connections). The in-house developed algorithm named PATCH was employed on the raw diffusion data to correct for cardiac and head motion artifacts and eddy currents.¹⁴ Diffusion Toolkit (www.trackvis.org) was used to calculate the diffusion tensor and FA. To generate the fiber tracks of the entire brain for each participant, fiber assignment by continuous tracking was employed using Diffusion Toolkit. The tracking algorithm started at the center of all voxels with FA >0.2 and ended when the fiber tracks left the brain mask or encountered voxels with FA <0.2, or when the turning angle exceeded 60°. Two regions were considered connected if the endpoints of the reconstructed streamline lay within both regions. For each participant, a weighted edge was constructed using the mean FA for each streamline and the number of reconstructed streamlines connecting 2 regions.¹⁵ Note that this

remains an indirect measure, as measuring directly the number of fibers or connection strength as a true measure is currently not possible with tractography techniques in general.¹⁶ None of the current techniques is capable of reconstructing individual nerve fibers or fiber bundles and as such, interpreting the number of reconstructed streamlines as a true measurement of the number of actual fibers is inappropriate.¹⁶ The connection strength was further normalized by the average of these volumes to correct for the different sizes of the AAL regions and different brain sizes.¹⁷ This resulted in an undirected weighted 90 × 90 matrix for each participant.

Graph theory analysis. Graph theoretical network measures were computed using the Brain Connectivity Toolbox.¹⁸ Basic network measures include density and total network strength. Density is defined as the total number of edges in a network observed divided by the possible number of edges. Total network strength represents the sum of weighted edges of a network. Next, we calculated global and local efficiency. Efficiency between 2 regions is expressed as the inverse of the shortest path length between 2 regions. The shortest path length refers to the minimum number of weighted connection between 2 regions. Global efficiency of the network is defined as the average of efficiency for all node pairs. The local efficiency for each node is the global efficiency of all direct

Table 1 Baseline characteristics of the study population

	Dementia (n = 32)	No dementia (n = 404)	p Values
Age, y, mean (SE)	74.2 (6.7)	64.5 (8.6)	<0.001 ^a
Sex, male, n (%)	18 (56)	219 (54)	0.969 ^b
Low education, n (%) ^c	9 (22)	36 (9)	0.039 ^b
MMSE, median (range)	27 (25-28)	29 (27-30)	<0.001 ^d
Depressive symptoms, mean (SE)	12.7 (8.6)	11.1 (9.6)	0.356 ^a
Vascular risk factors			
Hypertension, n (%)	28 (88)	288 (71)	0.077 ^b
Diabetes, n (%)	7 (22)	53 (13)	0.264 ^b
Smokers, n (%) ^e	23 (72)	279 (69)	0.894 ^b
Hypercholesterolemia, n (%)	17 (53)	174 (43)	0.358 ^b
BMI, mg/kg ² , mean (SE)	26.2 (3.6)	27.2 (4.2)	0.169 ^a
Physical activity, median (range)	47.8 (28.8-76.8)	57 (34.5-84.6)	0.112 ^a
Neuroimaging			
WMH, mL, median (range)	13.1 (7.8-29.1)	6.0 (3.2-15.4)	<0.001 ^a
Lacunes, presence, n (%)	10 (31)	87 (22)	0.293 ^b
Microbleeds, presence, n (%)	5 (16)	62 (15)	1.000 ^b
WM volume, mL, mean (SE)	425.0 (59.3)	470.4 (65.2)	<0.001 ^a
GM volume, mL, mean (SE)	586.9 (78.3)	634.4 (64.9)	<0.001 ^a
Fractional anisotropy, mean (SE)	0.38 (0.05)	0.40 (0.03)	<0.001 ^a
Mean diffusivity	9.1 × 10 ⁻⁴ (5.4 × 10 ⁻⁵)	8.8 × 10 ⁻⁴ (5.4 × 10 ⁻⁵)	<0.001 ^a
Hippocampal volume, mL, mean (SE)	5.9 (1.1)	6.8 (0.9)	<0.001 ^a
Global efficiency	3.2 × 10 ⁻³ (6.9 × 10 ⁻⁴)	4.0 × 10 ⁻³ (8.3 × 10 ⁻⁴)	<0.001 ^a

Abbreviations: BMI = body mass index; GM = gray matter; MMSE = Mini-Mental State Examination; WM = white matter; WMH = white matter hyperintensities.

^aIndependent samples t test.

^bχ² test.

^cLow education refers to primary education.

^dMann-Whitney U test.

^eSmoker includes current and ex-smokers.

Table 2 Correlations between SVD markers and network measures

	WMH	Lacunes	Microbleeds	WM volume
Density	-0.59	-0.31	-0.25	0.57
Total network strength	-0.60	-0.30	-0.23	0.63
Global efficiency	-0.62	-0.32	-0.25	0.59
Local efficiency	-0.58	-0.28	-0.19	0.57

Abbreviations: SVD = small vessel disease; WM = white matter; WMH = white matter hyperintensities.

Data represent Pearson correlations. MRI markers for SVD were strongly associated with network measures in the full set of participants ($n = 436$). All correlations are significant ($p < 0.05$, Bonferroni-corrected).

neighbors of that node. The global efficiency reflects the extent to which information communication is globally integrated in the network, whereas the local efficiency measures the segregation and specialization within a network.

Statistical analysis. Person-years at risk were calculated from date of the baseline assessment until onset of dementia, death, or date of the follow-up assessment. Group differences in baseline characteristics were tested by independent t test, χ^2 test, or Mann-Whitney U test, when appropriate (table 1).

Cox proportional regression analyses were used to obtain hazard ratios (HR) for each risk factor and for each MRI parameter (GM, WM, WMH volume, lacunes, microbleeds, FA, and MD), adjusted for age, sex, education, and baseline Mini-Mental State Examination (MMSE). Next, multivariable forward stepwise Cox regression model was performed with age, sex, education, and baseline MMSE as fixed predictors when entering the significant predictors (with $p < 0.05$ for entry and $p > 0.1$ for removal). Patients who died or did not reach the endpoint were censored.

Penalized Cox regression with least absolute shrinkage and selection operator (Lasso) was chosen as a secondary analysis to confirm the findings from the multivariable approach. This method is useful for selecting predictors from a set of potential predictors, reduces overfitting, and minimizes the effects of outliers, especially in datasets with a large number of variables with respect to the number of events. Variables were standardized when appropriate before performing the Lasso model and the tuning parameter was selected through a 10-fold cross-validation. Statistical analyses were done using R (<http://www.r-project.org>).

RESULTS Baseline characteristics are displayed in table 1. Mean follow-up of participants was 5.2 years

Table 3 Differences in network measures between dementia and no dementia groups at baseline

	Dementia ($n = 32$)	No dementia ($n = 404$)	p Values
Density	0.10 (0.02)	0.12 (0.01)	0.146
Total network strength	0.05 (0.01)	0.07 (0.02)	0.014
Global efficiency	3.2×10^{-3} (6.9×10^{-4})	4.0×10^{-3} (8.3×10^{-4})	0.042
Local efficiency	3.3×10^{-3} (6.2×10^{-4})	3.9×10^{-3} (7.0×10^{-4})	0.074

Data represent mean (SD). The dementia group showed lower total network strength and global and local efficiency at baseline as compared with the no dementia group. Each network measure was corrected for age, sex, educational level, and Mini-Mental State Examination using multiple regression technique. Permutation testing (with 10,000 iterations) was used to create a null distribution of effects under the null hypothesis, which then was used to calculate the p value.

(SD 0.9). A total of 32 participants developed dementia (20 with AD, 9 with VaD, and 3 with possible AD with etiologically mixed presentation), resulting in a 5.5-year cumulative dementia risk of 9.4% (95% confidence interval [CI] 5.6–13.0). At baseline, mean age of participants who developed dementia was 74.2 years (SD 6.7) with median baseline MMSE of 27 (range 25–28), and 64.5 years (SD 8.6) with median baseline MMSE of 29 (range 27–30) for those who did not develop dementia. Those who developed dementia had a higher WMH volume, smaller WM, GM, and hippocampal volume, lower FA, and higher MD compared to those who did not develop dementia (table 1).

MRI markers for SVD were associated with network measures (density, network strength, global efficiency, and local efficiency) (table 2; $p < 0.05$, Bonferroni-corrected). Furthermore, we analyzed the network measures in the dementia group ($n = 32$) and the no dementia group ($n = 404$). Each network measure was corrected for confounding factors (age, sex, educational level, and MMSE score) using multiple regression technique. Permutation testing (with 10,000 iterations) was then used to create a null distribution of effects under the null hypothesis, which was then used to calculate the p value. Although the density of the network did not differ between the groups (e.g., the number of edges within the network was not different), the dementia group showed lower total network strength and global efficiency at baseline as compared with the no dementia group (table 3).

Higher age (HR 1.1, 95% CI 1.1–1.2, $p < 0.001$) and lower MMSE scores (HR 0.8, 95% CI 0.6–0.9, $p = 0.015$) were associated with increased risk of incident all-cause dementia. Lower global efficiency (HR per decrease of 1 SD 0.6, 95% CI 0.4–0.9, $p = 0.018$) and lower hippocampal volume (HR per decrease of 1 SD 0.6, 95% CI 0.4–0.9, $p = 0.004$) were associated with increased risk of incident all-cause dementia. These predictors remained significant in a multivariable model (table 4; model 2). In contrast, none of the other MRI parameters was a predictor of dementia. The model was rerun with inclusion of a multiplicative interaction term for hippocampal volume \times global efficiency, which was not significant. Lasso regression method confirmed the identification of these neuroimaging variables (hippocampus volume and global efficiency) as predictors for incident all-cause dementia (figure).

DISCUSSION We have shown that patients with lower network efficiency (indicated by lower global efficiency) at baseline had an increased risk of incident all-cause dementia during 5 years of follow-up

Table 4 Cox proportional hazard regression analysis of predictors at baseline for all-cause dementia risk

	All-cause dementia (n = 32), HR (95% CI); p Value	
	Model 1	Model 2
Age	1.14 (1.08-1.21); <0.001 ^a	1.10 (0.91-1.17); 0.002 ^a
Sex	0.94 (0.47-1.89); 0.857	1.01 (0.50-2.05); 0.945
Education	0.69 (0.27-1.78); 0.446	0.72 (0.28-1.85); 0.497
MMSE	0.77 (0.64-0.95); 0.015 ^a	0.80 (0.65-0.90); 0.043 ^a
Depressive symptoms	1.02 (0.98-1.06); 0.347	—
Vascular risk factors		
Hypertension	1.22 (0.42-3.55); 0.719	—
Diabetes	1.29 (0.54-1.06); 0.561	—
Smokers ^b	1.10 (0.60-2.03); 0.753	—
Hypercholesterolemia	1.22 (0.59-2.54); 0.588	—
BMI ^c	0.77 (0.48-1.15); 0.183	—
Physical activity ^c	0.86 (0.58-1.29); 0.468	—
Neuroimaging		
WMH ^c	1.27 (0.81-2.01); 0.201	—
Lacunes, presence	0.87 (0.39-1.92); 0.730	—
Microbleeds, presence	0.56 (0.62-1.54); 0.264	—
WM volume ^c	0.74 (0.49-1.12); 0.160	—
GM volume ^c	0.60 (0.51-1.25); 0.327	—
Fractional anisotropy	0.79 (0.60-1.05); 0.101	—
Mean diffusivity	0.92 (0.63-1.34); 0.658	—
Hippocampal volume ^c	0.59 (0.42-0.85); 0.004 ^a	0.59 (0.41-0.85); 0.004 ^a
Global efficiency ^c	0.63 (0.42-0.96); 0.030 ^a	0.63 (0.42-0.96); 0.032 ^a

Abbreviations: BMI = body mass index; CI = confidence interval; GM = gray matter; HR = hazard ratio; MMSE = Mini-Mental State Examination; WM = white matter; WMH = white matter hyperintensities.

Model 1: adjusted for age, sex, education, and MMSE. Model 2: multivariable model including significant predictors from model 1.

^ap < 0.05.

^bSmoker includes current or ex-smokers.

^cPer standard deviation difference from the mean.

in a cohort of elderly participants with cerebral SVD. In addition, hippocampal volume was a significant predictor for incident dementia.

In contrast to the association of network efficiency with risk of dementia, conventional MRI markers including brain volume, lacunes, WMH, microbleeds, and DTI measures (FA and MD) were not associated with dementia risk while adjusting for age, sex, education, and MMSE. These individual markers have been associated previously with cognitive impairment and dementia.^{19,20} In a cross-sectional study, the association of these SVD markers with cognitive impairment might at least in part be mediated by damage to the WM network.⁴ Their lack of association with risk of dementia after controlling for network efficiency suggests that their effects may be mediated via network disruption.⁴

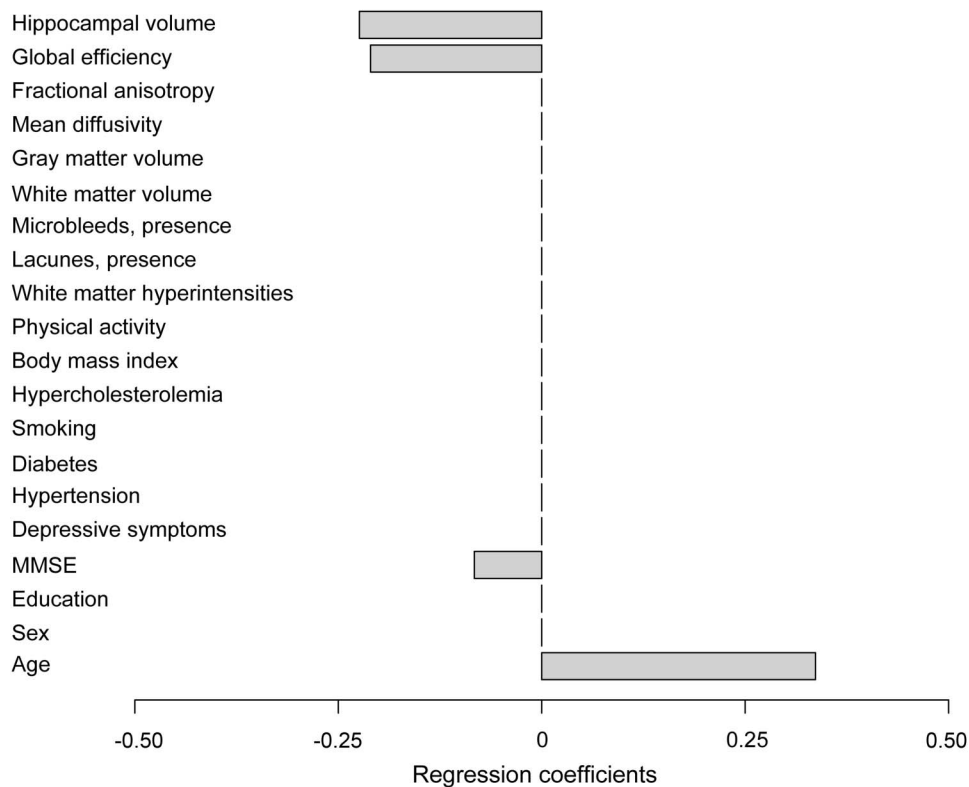
In our study, AD and VaD were pooled to all-cause dementia, because the aim of the study was to predict development of cognitive decline to a level of dementia, irrespective of the clinically diagnosed etiology. Although the participants were selected based on the presence of SVD on neuroimaging, most of the cases converting to dementia were of the AD type. These participants without dementia at baseline could therefore actually be in a preclinical stage of AD pathology, where SVD would be a coexisting factor or may interact with AD pathology.

Nevertheless, these findings suggest that structural network measures might capture the various factors that influence cognitive function, such as SVD-related lesions and AD pathology.²¹ Perhaps participants with lower network efficiency could be more vulnerable to additional pathology, contributing to further network breakdown and thereby having an increased risk for cognitive decline and eventually clinically evident dementia. Structural network efficiency might thus possibly serve as an early predictor of dementia.

Strengths of this study include its longitudinal design in a study population showing various degree of SVD on neuroimaging, collection of the data in a single center, a high follow-up rate, extensive adjustments for other variables, and inclusion of an additional analysis using Lasso method to confirm the multivariable analysis.

Several methodologic issues should be addressed. Accurate clinical diagnosis of AD and VaD based on clinical assessment and MRI can be difficult, because of a considerable overlap between these dementia types regarding the pathologic and clinical features.² Also, specific associations between neuroimaging predictors and particular dementia syndromes cannot be investigated due to the limited cases of dementia. An interesting future question would be to examine the predictive relations between potential predictors and specific dementia syndromes. Furthermore, information about other predictors, such as *APOE* status and CSF biomarkers, were lacking, which might have improved the prediction model for dementia. The relatively low number of cases of dementia raises the question whether the study sample is representative for a typical population at risk. Compared with another study in participants with SVD,²² the number of cases of dementia was lower (32 cases among 436 participants after 5 years of follow-up vs 90 out of 588 after 3 years), probably due to the fact that our study consisted of a younger population with less severe WMH volume at baseline. However, the incidence of 14.3 per 1,000 person-years in our study was higher than the incidence of 8.1 years per 1,000 person-years in a population-based study,² in which the traditional SVD markers (e.g., lacunes) were found predictive. This is probably

Figure Regression coefficients from the least absolute shrinkage and selection operator (Lasso) regression method



Neuroimaging variables determined as predictors for incident all-cause dementia were global efficiency and hippocampal volume. MMSE = Mini-Mental State Examination.

due to the fact the median WMH volume in our study was higher. Our study has a high generalizability to patients aged between 50 and 85 years with SVD on neuroimaging in a general neurology clinic. Nevertheless, it would be interesting to examine whether the network measures would also be predictive in other study populations. Furthermore, the tractography technique and the parcellation scheme applied in this study have several limitations, such as failure in reconstructing tracts in complex WM architecture, identifying long distance tracts due to noise, partial volume effects, and unequal-sized brain regions using AAL regions.^{23,24} Although these techniques are widely used and robust in terms of identifying major WM tracts, other tractography techniques, parcellation schemes, and construction of fiber tracts at high resolution are warranted to verify these findings. It should also be emphasized that there is currently no technical advancement capable of identifying the quantitative degree of WM connectivity as a true measure.²⁵ Despite these limitations, network efficiency based on indirect measures of WM connectivity provides biologically relevant information not present in other imaging markers.

WM network efficiency and hippocampal volume were both related to risk of incident all-cause

dementia in elderly participants with SVD. These results support a role of WM network disruption playing in pivotal role in the genesis of dementia and highlight the potential of a disease marker to identify patients at risk for dementia at an early stage over the conventional MRI markers.

AUTHOR CONTRIBUTIONS

Dr. Tuladhar: involved in data collection, analysis and interpretation of data, and drafting and revising the manuscript. Dr. van Uden: involved in data collection and in revising the manuscript. Dr. Rutten-Jacobs: involved in analysis and revising the manuscript. Dr. Lawrence: involved in analysis and revising the manuscript. Dr. van der Holst: involved in data collection, data analysis, and revising the manuscript. Dr. van Norden: involved in study concept and design, data collection, and revising the manuscript. Dr. de Laat: involved in study concept and design, data collection, and revising the manuscript. Dr. van Dijk: involved in study concept and design and revising the manuscript. Dr. Claassen: involved in data collection, data analysis, and revising the manuscript. Prof. Kessels: involved in data collection, data analysis, and revising the manuscript. Prof. Markus: involved in data analysis and revising the manuscript. Prof. Norris: involved in study concept and design and revising the manuscript. Dr. de Leeuw: involved in study concept and design, analysis and interpretation of data, revising the manuscript, study supervision, and obtaining funding.

STUDY FUNDING

Supported by a VIDI innovational grant from the Dutch Organization for Scientific Research (grant 016.126.351), MIRA Institute for Biomedical Technology and Technical Medicine, University of Twente, and Internationale Stichting Alzheimer Onderzoek.

DISCLOSURE

A. Tuladhar, I. van Uden, and L. Rutten-Jacobs report no disclosures relevant to the manuscript. A. Lawrence is supported by a project grant from Alzheimer's Research UK. H. van der Holst, A. van Norden, and K. de Laat report no disclosures relevant to the manuscript. E. van Dijk received a personal fellowship from the Dutch Brain Foundation (H04-12; F2009(1)-16). J. Claassen and R. Kessels report no disclosures relevant to the manuscript. H. Markus is supported by an NIHR Senior Investigator award and by the Cambridge Universities Trust NIHR Comprehensive Biomedical Research Centre. D. Norris and F. de Leeuw report no disclosures relevant to the manuscript. Go to Neurology.org for full disclosures.

Received August 17, 2015. Accepted in final form November 16, 2015.

REFERENCES

1. Wardlaw JM, Smith EE, Biessels GJ, et al. Neuroimaging standards for research into small vessel disease and its contribution to ageing and neurodegeneration. *Lancet Neurol* 2013;12:822–838.

Comment: Network disruption as a common framework for factors contributing to dementia

There is mounting evidence that large-scale functional brain networks are fundamental to the pathophysiology of dementing illnesses.¹ Functional networks require intact white matter, and small vessel disease (SVD) may disrupt this infrastructure. Tuladhar et al.² conducted an analysis of imaging biomarkers as predictors of all-cause dementia in a prospective hospital-based cohort of patients with presumed evidence of SVD. The imaging biomarkers included white matter network-based graph theoretical metrics (e.g., global network efficiency), white matter volume, gray matter volume, hippocampal volume, manually segmented white matter hyperintensity volume, and presence/absence of lacunes and microbleeds.

The authors found that measures of SVD were correlated with network measures indicating shared information between these metrics. However, they demonstrate that among the imaging biomarkers studied, hippocampal volume and global network efficiency were the only imaging predictors of all-cause dementia in their cohort. This result suggests that one way by which factors associated with SVD contribute to dementing pathophysiology is via their effects on large-scale networks.

While diffusion MRI-based tractography may not be able to reproduce true structural connectivity faithfully,³ the current study demonstrates that this technique can create biologically relevant models of white matter networks that contain information that is absent in traditional markers of white matter integrity. A key piece of information that is lacking in traditional measures of white matter integrity is the importance of lesion location to global network function. For example, strategic insults located in pathways connecting hubs of high importance will be modeled by traditional biomarkers as having the same effect as lesions of little importance to global network communication. However, measures sensitive to these lesions that can be used to generate network models will be sensitive to strategic differences in lesion location.

This study supports the utility of using network measures as biomarkers of pathophysiologic processes related to the development of dementia.

1. Jones DT, Knopman DS, Gunter JL, et al. Cascading network failure across the Alzheimer's disease spectrum. *Brain* Epub 2015 Nov 19.
2. Tuladhar AM, van Uden IWM, Rutten-Jacobs LC, et al. Structural network efficiency predicts conversion to dementia. *Neurology* 2016;86:1112–1119.
3. Reveley C, Seth AK, Pierpaoli C, et al. Superficial white matter fiber systems impede detection of long-range cortical connections in diffusion MR tractography. *Proc Natl Acad Sci USA* 2015;112:E2820–E2828.

David Thomas Jones, MD

From the Departments of Neurology and Radiology, Mayo Clinic, Rochester, MN.

Study funding: No targeted funding reported.

Disclosure: The author reports no disclosures relevant to the manuscript. Go to Neurology.org for full disclosures.

2. Vermeer SE, Prins ND, den Heijer T, Hofman A, Koudstaal PJ, Breteler MM. Silent brain infarcts and the risk of dementia and cognitive decline. *N Engl J Med* 2003;348:1215–1222.
3. Firbank MJ, Burton EJ, Barber R, et al. Medial temporal atrophy rather than white matter hyperintensities predict cognitive decline in stroke survivors. *Neurobiol Aging* 2007;28:1664–1669.
4. Lawrence AJ, Chung AW, Morris RG, Markus HS, Barrick TR. Structural network efficiency is associated with cognitive impairment in small-vessel disease. *Neurology* 2014;83:304–311.
5. Erkinjuntti T. Subcortical vascular dementia. *Cerebrovasc Dis* 2002;13(suppl 2):58–60.
6. de Laat KF, Tuladhar AM, van Norden AG, Norris DG, Zwiers MP, de Leeuw FE. Loss of white matter integrity is associated with gait disorders in cerebral small vessel disease. *Brain* 2011;134:73–83.
7. American Psychiatric Association. Diagnostic and statistical manual of mental disorders, 4th ed. Washington, DC: American Psychiatric Association; 2000.
8. McKhann GM, Knopman DS, Chertkow H, et al. The diagnosis of dementia due to Alzheimer's disease: recommendations from the National Institute on Aging-Alzheimer's Association workgroups on diagnostic guidelines for Alzheimer's disease. *Alzheimers Dement* 2011;7:263–269.
9. Roman GC, Tatemichi TK, Erkinjuntti T, et al. Vascular dementia: diagnostic criteria for research studies. Report of the NINDS-AIREN International Workshop. *Neurology* 1993;43:250–260.
10. van Norden AG, de Laat KF, Gons RA, et al. Causes and consequences of cerebral small vessel disease: the RUN DMC study: a prospective cohort study: study rationale and protocol. *BMC Neurol* 2011;11:29.
11. Gons RA, Tuladhar AM, de Laat KF, et al. Physical activity is related to the structural integrity of cerebral white matter. *Neurology* 2013;81:971–976.
12. Tzourio-Mazoyer N, Landeau B, Papathanassiou D, et al. Automated anatomical labeling of activations in SPM using a macroscopic anatomical parcellation of the MNI MRI single-subject brain. *Neuroimage* 2002;15:273–289.
13. Smith SM, Jenkinson M, Woolrich MW, et al. Advances in functional and structural MR image analysis and implementation as FSL. *Neuroimage* 2004;23(suppl 1):S208–S219.
14. Zwiers MP. Patching cardiac and head motion artefacts in diffusion-weighted images. *Neuroimage* 2010;53:565–575.
15. Lo CY, Wang PN, Chou KH, Wang J, He Y, Lin CP. Diffusion tensor tractography reveals abnormal topological organization in structural cortical networks in Alzheimer's disease. *J Neuroscience* 2010;30:16876–16885.
16. Jones DK, Knosche TR, Turner R. White matter integrity, fiber count, and other fallacies: the do's and don'ts of diffusion MRI. *Neuroimage* 2013;73:239–254.
17. Brown JA, Terashima KH, Burggren AC, et al. Brain network local interconnectivity loss in aging APOE-4 allele carriers. *Proc Natl Acad Sci USA* 2011;108:20760–20765.
18. Rubinov M, Sporns O. Complex network measures of brain connectivity: uses and interpretations. *Neuroimage* 2010;52:1059–1069.
19. van Norden AG, de Laat KF, van Dijk EJ, et al. Diffusion tensor imaging and cognition in cerebral small vessel

- disease: the RUN DMC study. *Biochim Biophys Acta* 2012;1822:401–407.
20. Prins ND, Scheltens P. White matter hyperintensities, cognitive impairment and dementia: an update. *Nat Rev Neurol* 2015;11:157–165.
 21. Reijmer YD, Leemans A, Brundel M, Kappelle LJ, Biessels GJ; Utrecht Vascular Cognitive Impairment Study G. Disruption of the cerebral white matter network is related to slowing of information processing speed in patients with type 2 diabetes. *Diabetes* 2013;62:2112–2115.
 22. Verdelho A, Madureira S, Ferro JM, et al. Physical activity prevents progression for cognitive impairment and vascular dementia: results from the LADIS (Leukoaraiosis and Disability) study. *Stroke* 2012;43:3331–3335.
 23. Zalesky A, Fornito A. A DTI-derived measure of cortico-cortical connectivity. *IEEE Trans Med Imaging* 2009;28:1023–1036.
 24. Sporns O. Contributions and challenges for network models in cognitive neuroscience. *Nat Neurosci* 2014;17:652–660.
 25. Reveley C, Seth AK, Pierpaoli C, et al. Superficial white matter fiber systems impede detection of long-range cortical connections in diffusion MR tractography. *Proc Natl Acad Sci USA* 2015;112:E2820–E2828.



Register Today for the 2016 AAN Annual Meeting

Register today for the innovative new AAN Annual Meeting, set to take place Friday, April 15, through Thursday, April 21, 2016, at the Vancouver Convention Centre in Vancouver, BC, Canada. The money-saving early registration deadline is March 24, 2016. Visit AAN.com/view/AM16 to learn more and register today!

AAN Guideline Recommends Removal of Player if Concussion Suspected

Athletes who are suspected of having a concussion should be removed from the game immediately and not be returned until assessed by a licensed health care professional trained in diagnosing and managing concussion. That is one of the recommendations of the American Academy of Neurology's highly accessed evidence-based guideline for evaluating and managing athletes with concussion.

Share this information with patients, families, coaches, athletic trainers, and colleagues. Visit AAN.com/concussion for all your concussion resources:

- Read the published guideline
- Access PDF summaries for clinicians, coaches, athletic trainers, and patients
- Download the slide presentation
- Review a clinical example
- Download the Academy's convenient mobile app, **Concussion Quick Check**, to quickly help coaches and athletic trainers recognize the signs of concussion.

For more information, contact Julie Cox at jcox@aan.com or (612) 928-6069.